

(K 4075) JAPAN  
1995.

## DISPERSION DECREASING FIBRES FOR SOLITON GENERATION AND TRANSMISSION LINE LOSS COMPENSATION

D.J. RICHARDSON, R.P. CHAMBERLAIN, L. DONG and D.N. PAYNE  
Optoelectronics Research Center,  
Southampton University,  
Southampton, S017 1BJ.  
United Kingdom.

### 1. Introduction

The idea of varying the axial distribution of dispersion along a length of optical fibre as a means of manipulating and controlling the soliton supporting nature of the fibre and thereby the characteristics of soliton pulses propagating through the medium has been around for some while [1,2]. A number of specific applications have been suggested in particular techniques for bright and dark soliton generation [3,4], pulse compression [5] and most notably techniques for high frequency soliton transmission [1]. The experimental realisation of most of these techniques however has been hindered by difficulties in the reliable fabrication of dispersion varying fibres. A technique for the fabrication of such fibres was first developed by workers at General Physics Institute, Moscow [6]. Control of the waveguide dispersion was achieved by active control of fibre diameter during the pull. Fibre lengths of up to 2 km were fabricated and successfully used in the first experimental demonstrations of high frequency (>60 GHz) bright soliton generation [3,7] and pulse compression [5,8]. Subsequent to these first experimental results a number of other groups have commenced fabrication programs on such fibres, extending the techniques to fibre lengths of 40 km. In this presentation we describe our latest achievements in Dispersion Decreasing Fibre (DDF) fabrication and report on two applications of the technology. Firstly, we describe a robust, diode-pumped, 40 GHz bright soliton transmitter [9,10], and secondly we demonstrate loss compensation in a 38km loss-matched dispersion varying fibre [11].

### 2. Dispersion Decreasing Fibre fabrication

As is well known the total chromatic dispersion of a fibre  $D_{Tot}$  can be closely approximated as the sum of two components  $D_{Tot} = D_M + D_W$ , where  $D_M$  is the material dispersion and  $D_W = (\Delta n / \lambda) \cdot (V d^2(BV) / dV^2)$ , the waveguide dispersion.  $\Delta n$  is the index difference and  $B$  and  $V$  are the normalised propagation constant and frequency respectively [12]. Controlled variation of the waveguide characteristics along the fibre

length can therefore result in controlled dispersion variation. In order to continuously vary the waveguide dispersion along a section of fibre one needs to change one of the waveguide parameters along its length. By far the most convenient parameter to vary is the core diameter- and hence the effective V-value since this can be done during the fibre draw and does not require special preform design. What is needed however, is accurate fibre diameter control during the pulling process and the production of highly length-homogenous preforms.

Our fibres were pulled on a commercial 7m fibre pulling tower on which the fibre diameter was stabilised by active control of the fibre pulling speed. Computer software was developed to continuously and controllably vary the fibre diameter to follow any required diameter variation. The control loop feedback parameters were optimised over the full range of required pull speeds 30-80 m/min, enabling RMS diameter errors  $<0.2 \mu\text{m}$  over the diameter range of 75 - 150  $\mu\text{m}$ , with negligible diameter offset error ( $<0.1 \mu\text{m}$ ). A (typical) plot of set diameter and experimentally determined fibre difference from the set value are shown in Fig.1 illustrating the quality of the diameter control obtained for the 20 km loss compensating dispersion decreasing fibre (LCDDF1) described in Section 4.

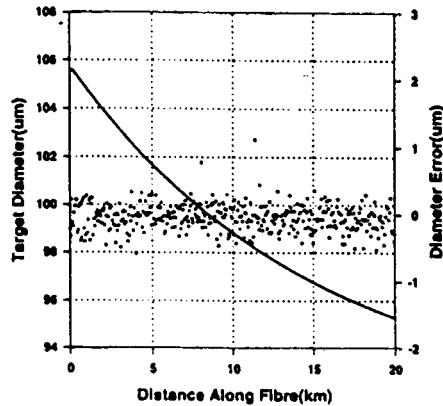


Fig.1 Diameter variation and measured diameter offset from set diameter along the fibre length for a 20 km loss compensating dispersion decreasing fibre (LCDDF1).

In order to fabricate useful/interesting fibres at 1550 nm one needs to be able to make the waveguide dispersion opposite in sign, and equal, or greater to in magnitude, to the material dispersion ( $\approx 20 \text{ ps/nm/km}$  at 1550 nm). This can be achieved either by using a simple step index design with an  $\text{NA} > 0.15$ , or by going to a more complex refractive index profile e.g. a dispersion shifted design. In Fig.3 we plot the experimentally determined variation in total dispersion as a function of fibre diameter obtained using the step refractive index profile shown in Fig.4 illustrating that both anomalous and normally dispersive, dispersion decreasing fibres are possible for diameter variations of order 30%. Note however that care has to be taken in the normal case to avoid bend loss effects at 1550nm due to the low cut-off wavelength. The effective



allow compatibility with state of the art, high data rate electronic signals [3]. In this section we report on the development and performance of a diode-driven, ultra-low jitter, 30-40 GHz soliton source with potential for telecommunication applications. We report the results of pulse propagation measurements of 35 GHz repetition rate, 5ps pulses over a 205 km dispersion shifted fibre (DSF) transmission line [15] demonstrating for the first time that pulse trains from such sources can be transmitted with low distortion over terrestrial distances. Finally, we describe results on the all-optical modulation of pulses from such a source which illustrate that synchronisation, modulation and electrical detection issues specific to the use of such high frequency pulse sources can be overcome to give error free operation.

The source configuration (Fig.3) consists of three principal components: an optical beat-signal source, an  $\text{Er}^{3+}/\text{Yb}^{3+}$  optical power amplifier and a dispersion varying fibre section. In order to obtain a low timing jitter beat signal we used a 20 GHz amplitude modulator tuned to a transmission null and driven at 17.5 GHz to obtain 35 GHz sinusoidal modulation of the output from a DFB laser diode. Two equal amplitude frequency components separated by 35 GHz are obtained with almost no component at the carrier wavelength. The dispersion decreasing fibre section consisted of 2 km of DSF to spectrally enrich the input beat signal [7], and an 8 km DDF. The DDF dispersion followed a hyperbolic profile at 1550 nm tapering along the 8 km length from 13.75 to 2.75 ps (nm.km). The profile and output dispersion were chosen so as to reduce the absolute physical length of fibre required to obtain high quality, adiabatic 40 GHz pulse generation at an MSR of 5:1, whilst maintaining a practical optical power requirement on the input beat signal (80 mW).

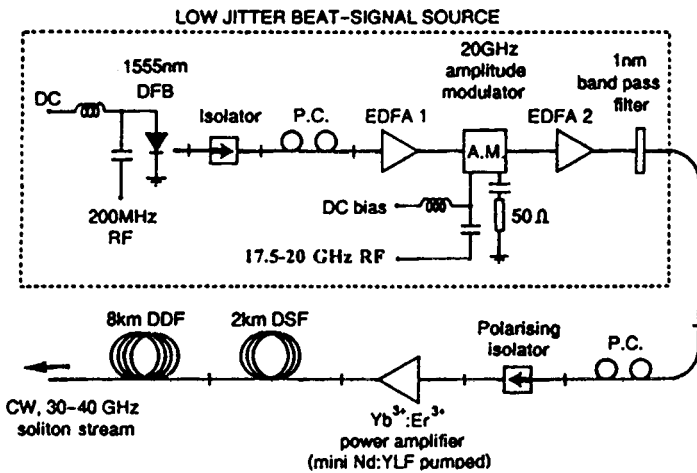


Fig.3 Schematic of diode-driven, stabilised 40 GHz bright soliton source.

The source was tested under a wide range of input powers and beat frequencies in the range 32-40 GHz. Transform-limited, soliton pulses of durations 4.5-6.5 ps were obtained for input beat signal powers <20 dBm within the wavelength range of the

available diodes 1547-1563nm. A typical autocorrelation function (ACF) and spectrum of a 35 GHz pulse train at the source output are shown in Fig.6a.

Pulse propagation experiments using the source were performed over a transmission line incorporating four  $\approx 50$  km spans of dispersion shifted fibre and 3 EDFAs [15]. The dispersion in the first and last two spans were  $D=0.07$  ps/(nm.km) and  $D=0.21$  ps/(nm.km) respectively. The ratio of soliton period to amplifier spacing was 3 over the first two DSF sections and 1 in the final two DSF spans. We therefore anticipate a strong departure from average soliton dynamics in the second half of the link resulting in the generation of significant dispersive wave radiation [16,17,18]. As expected the pulses were found to propagate with negligible distortion either temporally, or spectrally, over the first 100 km (see Figs.6b). Marked changes were however observed during propagation in the final two higher dispersion spans (Figs. 6c). In the time domain the pulses are found to propagate with reasonable stability, with little distortion other than a slight temporal narrowing and the appearance of a low-level, flat background ( $<5\%$ ) on the ACF at 205 km. However a modulation of the train spectral envelope is observed due to the constructive interference of dispersive wave radiation shed from the pulses within the final two DSF spans [18]. The depth and position of the spectral modulation and the appearance of the low-level ACF background component at 205 km is in good agreement with our numerical simulations of the system.

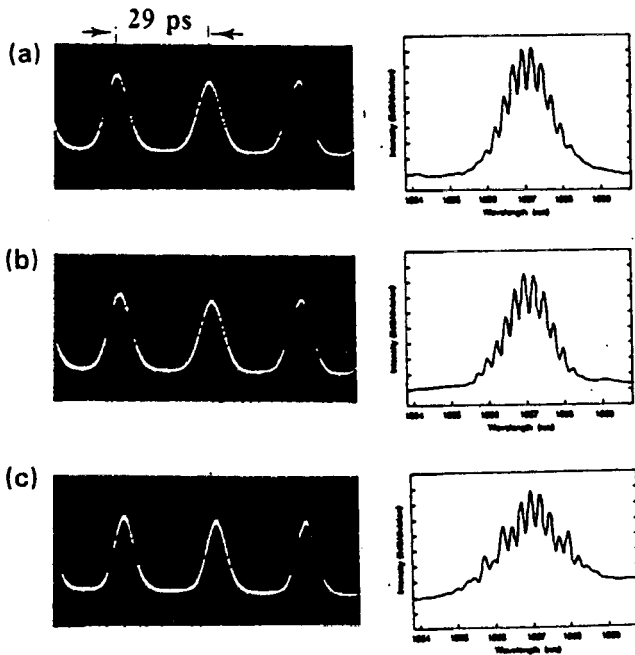


Fig.4 Autocorrelation and optical spectrum of 35 GHz pulse trains (a) at the system input,(b) after 100 km, (c) after 200 km.

Due to the low jitter beat signal seed source we were able to make direct electrical domain measurements on the pulse trains for the first time. The output pulse timing jitter was determined to be defined entirely by the phase noise of the modulator drive synthesizer (<300 fs). Furthermore, using electrical clock recovery circuits we have recently been able to synchronize a 6.4ps, 40 Gbit/s optical data stream to the output of the soliton source. (The 6.4ps pulses were generated using a gain-switched diode operating at 1545nm. The diode output was externally modulated at 10 Gbit/s, and the resulting signal multiplexed to 40 Gbit/s). We could then employ an all optical modulator (Kerr Gate) to encode data all-optically directly onto the beat signal soliton stream. Demultiplexing using a second clock recovery unit and EA modulator could then be performed enabling BER measurements on the four 10Gbit/s soliton data channels to be made. Error free operation, without a noise floor was readily obtainable with a power penalty of <1.5 dB (See Fig.5) [10].

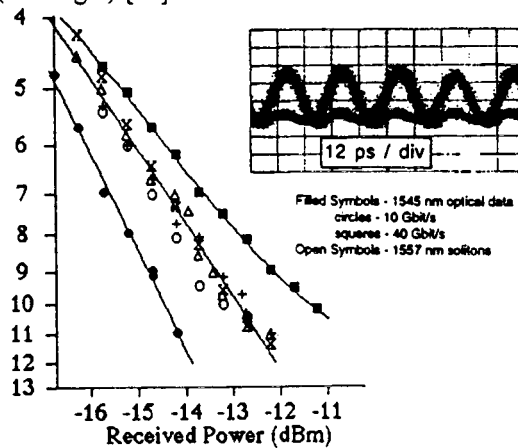


Fig.5 Eye diagram and BER rate curves for data encoded 40 Gbit/s data stream demultiplexed down to 10 Gbit/s illustrating error free all-optical modulation.

In conclusion, we have demonstrated a practical low-timing jitter, diode-driven, soliton source capable of operating in the range 30-40 GHz. Furthermore, we have performed the first long distance, multi-amplifier stage pulse transmission experiments using a beat-signal source, demonstrating high quality, transmission of 35 GHz, 5.2 ps pulses trains over a total distance of 205 km. Good pulse propagation characteristics were obtained despite the large amplifier separation of 50 km and strong violation of average soliton dynamics in the later half of the link. Transmission over considerably greater distances can be expected from an optimised system, with reduced dispersion variation and/or amplifier spacing. In addition, we have now demonstrated 40 Gbit/s, error free all optical data encoding onto the output of such sources illustrating for the first time that timing jitter, synchronisation issues associated with such source can readily be overcome. Note, also that 40 GHz modulators and chip sets are currently under development and in future should permit direct electro-optic modulation at 40 GHz [19]. The transmitter should enable a true assessment of the suitability of such sources for future high speed communication applications.

#### 4. Soliton loss compensation [11]

Soliton communication systems based on EDFAs offer enormous potential for high data rate transmission. However, a number of fundamental limitations associated with the periodic amplification process restrict the ultimate capacity of such systems. The first limitation arises due to the interaction of the solitons with the EDFA noise and manifests itself as timing jitter at the system output [20]. Fortunately, a number of techniques have been successfully developed to eliminate/reduce these particular effects [21,22]. The second limitation results directly from the periodic amplification process itself and arises once the soliton period ( $z_0$ ) of the pulses approaches the amplifier spacing ( $L_a$ ) [23]. In this regime the perturbation to the pulses due to the fibre loss becomes too severe resulting in a violation of 'average', or 'guiding centre', soliton dynamics and eventual decay of the pulses [16,17]. The perturbation can only be eliminated by ensuring that the dispersive and nonlinear effects balance at all points along the fibre despite the presence of background optical loss. This can be achieved either by using a distributed amplifier to cancel the local fibre loss [24], or by the use of a Loss Compensating Dispersion Decreasing Fibre (LCDDF) [1]. In the latter case the dispersion of the transmission fibre is made to fall exponentially along its length so as to exactly follow the decrease in optical intensity and hence the strength of the nonlinear interaction. An exact balance between the two effects at all points along the fibre is thus ensured. To date, most experimental effort has centred on the use of distributed amplifiers [24]. However, recently improved transmission of 1-2 ps pulses over a 40 km dispersion varying fibre span has been reported renewing interest in the LCDDF option [25]. Unfortunately, the dispersion variation of the fibre in these earlier experiments did not follow the loss profile so that although improved pulse transmission was indeed obtained, true loss compensation was not demonstrated. In this section we report the fabrication of a 38 km LCDDF with a dispersion profile closely matched to the fibre loss and demonstrate high quality soliton loss compensation over distances corresponding to  $>40 z_0$  (2ps pulses over a physical length of 20 km). (Note, we have also recently become aware that the authors of Ref.[9] have also now demonstrated true soliton loss compensation [26])

The LCDDF was fabricated from a step-index preform of NA=0.165, designed to give a 125  $\mu\text{m}$  single-mode fibre cut-off wavelength of 1310 nm. The preform had excellent homogeneity along its length. The required dispersion variation was obtained by tapering the fibre during the pulling process following a calibration procedure in which the dispersion, loss and mode-area variation with fibre diameter were determined. The exact fibre diameter variation required to achieve complete loss compensation over 38 km of fibre was evaluated for an input dispersion of 6.0 ps/(nm.km). A second order correction to compensate for the ~5% mode-area variation was included. The fibre was pulled in two sections (LCDDF1 and LCDDF2) that could either be used individually, or spliced together to give the full 38km span. The first section had a length of 20 km (dispersion variation based on fibre loss = 0.27 dB/km) and the second section a length of 18km (dispersion based on fibre loss = 0.26 dB/km). An OTDR plot of the actual fibre losses with the superposed design loss profiles are illustrated in Figs.6a and b. The

two glitches ( $\approx 0.3$  dB additional loss over lengths of 200m) observed in the measured

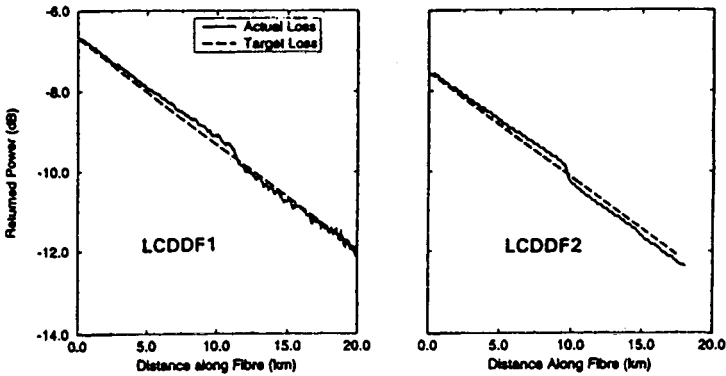


Fig.6 Experimental OTDR plot illustrating loss within LCDDF1 and LCDDF2 with superposed design loss profiles.

loss profiles were due to localised imperfections within the preform cladding and resulted in slight deviations from the desired form. The total deviation at any point within the fibres was however small ( $\leq \pm 0.2$  dB) with the average loss matching almost exactly in the case of LCDDF1 and within 0.2 dB within LCDDF2. The mismatch over the full 38 km was therefore 0.2 dB in 10.1 dB. The dispersion of LCDDF1 was set to vary exponentially from 6ps/nm.km at the input to 1.7 ps/nm.km at the output (corresponding to 5.4 dB loss) and from 1.7 ps/(nm.km) to 0.55 ps/(nm.km) (loss= 4.7 dB) in LCDDF2. The effective mode area varied from 47  $\mu\text{m}^2$  at the input to 50  $\mu\text{m}^2$  at the output. The required external fibre diameter variation was from 105-96  $\mu\text{m}$  in LCDDF1 and from 96  $\mu\text{m}$  to 92  $\mu\text{m}$  in LCDDF2. The local RMS dispersion along the fibre length was  $< 0.1$  ps/(nm.km) as determined from measurements of the RMS diameter error (0.18 $\mu\text{m}$ ). Measurements of the dispersion at the beginning and end of the two fibres along with average measurements along the two spans were in excellent agreement ( $\pm 0.15$  ps/nm/km) with our target values. The third order dispersion within the fibre was measured to be 0.053 ps/(nm<sup>2</sup>.km).

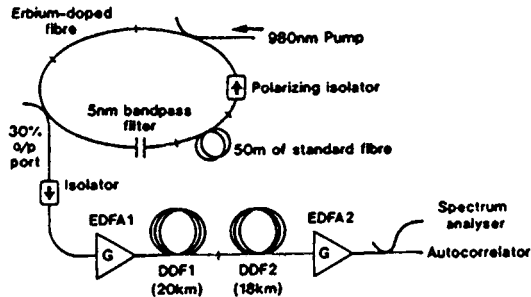


Fig.7 Experimental configuration used to examine soliton transmission characteristics of LCDDFs.



The experimental setup used to examine the pulse transmission characteristics of the LCDDF fibres is shown in Fig.7. Transform-limited pulses from a polarisation switch soliton laser with durations in the range 2.0-16 ps and tunable central wavelength in the range 1550-1565nm were input into EDFA1. By varying the gain of EDFA1 we could then vary the signal power launched into the LCDDF in order to match it to the fundamental soliton power for the fibre. EDFA2 was used to boost the signal level prior to autocorrelation and spectral measurements of the pulses at the system output. Initial experiments were performed using just the 20 km LCDDF1 with input pulses of 3.6ps and 2.0ps duration and central wavelengths around 1555 nm. In Fig.8a we present the input and output spectra and autocorrelations for the 3.6 ps pulse case where the launched pulse corresponds to that of the fundamental ( $N=1$ ) soliton. The transmission is seen to be excellent, the pulses are effectively indistinguishable in both the temporal and spectral domains indicating an excellent balance between dispersion and nonlinearity at all points along the LCDDF. The 20km fibre corresponded to an effective  $14 z_0$  in this instance. Similar results are presented for the 2.0ps case in Fig.8b. In this instance the pulses were observed to broaden slightly in the time domain from 2.0-2.2ps and to undergo slight spectral narrowing and deformation. In this instance the fibre corresponds to  $44 z_0$ . The loss compensation for this case is worse for the shorter duration pulses due to increased sensitivity to localised imbalances in nonlinearity and dispersion e.g. the glitch in Fig.6a as the soliton period is reduced at all points along the fibre.

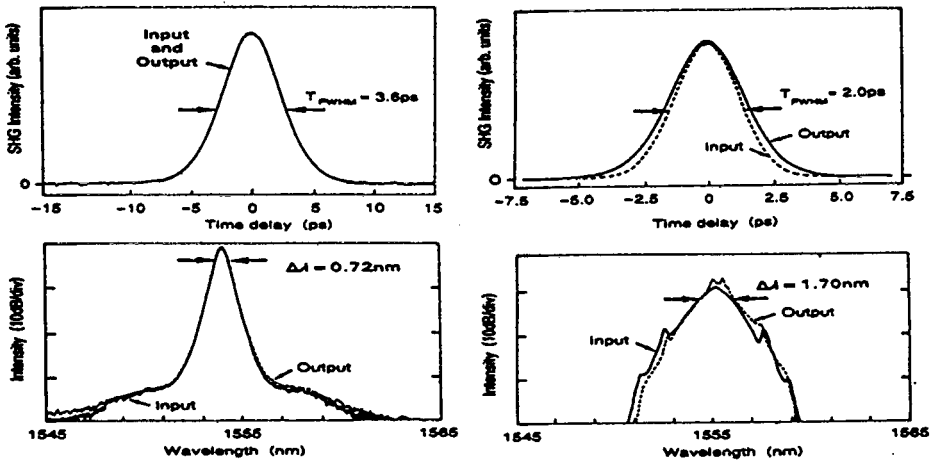


Fig.8 (a) ACF and spectra of 3.6 ps pulses at the input and output of LCDDF1 for the fundamental soliton input power, illustrating high-quality soliton loss compensation. The input and output autocorrelations are indistinguishable. The 20 km of fiber is equivalent to  $18 z_0$ . (Marked input pulse widths are deconvolved halfwidths.)  
 (b) Autocorrelation traces and spectra of 2.0 ps pulses at the input and output of LCDDF1 for a soliton input pulse power close to that of the fundamental. A 10% temporal broadening of the pulses is obtained and a small degree of spectral narrowing, lobing and shifting is observed. The 20 km of fiber is equivalent to  $44 z_0$ . (Marked input pulse widths are deconvolved halfwidths.)

The pulse transmission was also investigated as a function of input pulse power. At low powers the pulse simply broadened linearly with no spectral distortion, however as the pulse power was increased significant spectral distortion in the form of spectral narrowing and side-band generation was obtained along with a narrowing of the pulse in the time domain. The spectral distortion, reminiscent in form to the side band generation observed in simple soliton lasers, arises due to the imperfect balance between dispersion and nonlinearity at powers away from the fundamental and was anticipated from our numerical simulations of the system. As the fundamental power is approached the depth of spectral modulation reduces as a more complete balance of the nonlinear and dispersive effects is obtained along the entire fibre length. At input powers significantly higher than the fundamental the excess nonlinearity results in a compression of the pulses within the LCDDF. The soliton self-frequency shift then comes into play and leads to a spectral walk off of the pulses towards longer wavelengths.

The two LCDDF fibres were then spliced together to create a single 38 km span. The total fibre loss was 10.4 dB (splice loss = 0.1 dB). 3.5 ps pulse transmission over the full fibre span was then examined. The fibre span constituted  $\approx 18$  soliton periods in this instance. The autocorrelations and spectra of the pulses at the input, 20 km and 38 km are illustrated in Fig.9 for the input fundamental soliton case. It is seen that the pulses are successfully transmitted over the fibre length with minimal temporal distortion. A degree of spectral lobing is apparent at both 20 and 38 km due to the slight mismatch in nonlinearity and dispersion over the fibre length but the deviations in pulse form between input and output are still small. The maximum ripple is < 1dB over a 4nm bandwidth centred on the pulse illustrating the quality of the loss compensation.

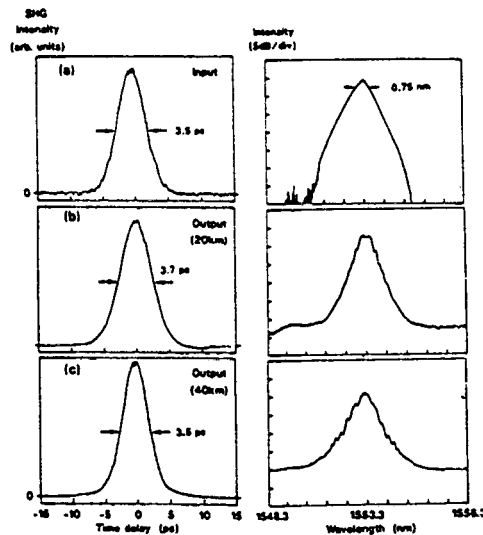


Fig.9 Spectra and autocorrelation plots of 3.5ps, N=1 solitons at (a) system input (0 km), (b) output of LCDDF1 (20 km) and (c) output of LCDDF2 (38 km). (Marked pulse widths are deconvolved pulse halfwidths.)

In conclusion we have demonstrated the fabrication of a 38 km long soliton loss compensating transmission fibre. An excellent match to the dispersion variation to loss profile has been obtained. The quality of the fibre has been confirmed in a series of single pulse propagation experiments. Fundamental soliton propagation of 2.0 ps pulses over  $\approx 44$  soliton periods (20 km) and 3.5ps pulses over 18 soliton periods (38 km) with minimal temporal and spectral deformation have been obtained. Our results clearly indicate that high-quality, soliton loss compensation can be achieved for a total distributed loss of  $\approx 10$  dB (40 km of fibre) and illustrate the possibility of amplifier spacings of  $\geq 40$  soliton periods for use in ultra-high speed transmission lines. Such span lengths (expressed in soliton periods) are around two orders of magnitude greater than those that can be envisaged for use in conventional soliton transmission systems limited by the constraints of average soliton dynamics. LCDDFs should therefore enable access to single channel system bit-rates well in excess of 40 Gbit/s providing the average dispersion of such fibres can be kept low enough to keep deleterious effects such as ASE induced timing jitter, soliton self frequency shift and soliton interaction effects to an acceptable level. It has also recently been pointed out that such fibres also seem offer advantages relative to conventional DSF in alleviating the problems due to soliton collisions in WDM based soliton systems [26]. Dispersion shifted fibres produced from a commercial preform typically exhibit a maximum variation in dispersion of  $\approx 0.2$  ps/(nm.km) along the entire pull length. With care improvements should be possible to enable  $\approx 0.1$  (ps/nm.km) accuracy along a 40 km fibre length and would enable a scaling of the dispersion characteristics of our fibre by  $\approx 1/5$ , thereby reducing the average dispersion to  $\approx 0.5$  ps/(nm.km), a value commensurate with current conventional soliton systems.

## 6. Conclusions

Technology for the fabrication of dispersion decreasing fibre has developed to the extent that accurate and controllable dispersion variation can readily be obtained over fibre lengths ranging from 10m to 40km. A wide range of applications have been demonstrated in the laboratory and a number extended to real system tests. Whether such components will ever find real world application remains to be seen, however, it is already evident that the technology has opened a significant new dimension to what can be achieved within the fibre environment, undoubtedly new applications will open up.

## 7. Acknowledgements

The authors would like to acknowledge the considerable contribution of A.D. Ellis, D.M. Spirit, T. Widdowson and W.A. Pender during collaborative work on the 40 Gbit/s soliton transmitter. The contribution of Pirelli (Cavi) through supply of preforms used within this work and that of Fibre-Core UK for advising and assisting in the use of the 7m pulling tower is gratefully acknowledged. In addition, the assistance of York Technology and Pirelli U.K. for providing access to dispersion measuring instrumentation is greatly appreciated. This work is funded in part by European Union RACE project R2015 "ARTEMIS", European Union ACTs project "MIDAS", EPSRC and the Royal Society.

## Sec.6: References

- 1 K. Tajima: *Opt. Lett.*, 12, 54-56, (1987).
- 2 H.H. Kuehl: *J. Opt. Soc. Am. B*, 5, 709-713 (1988).
- 3 P.V. Mamyshev, S.V. Chernikov, E.M. Dianov: *IEEE J. Quantum Electron.*, 27, 2347-2351, (1991).
- 4 D.J. Richardson, R.P. Chamberlain, L. Dong, D.N. Payne: *Electron. Lett.*, 30, 1326-1327, (1994).
- 5 S.V. Chernikov, P.V. Mamyshev: *J. Opt. Soc. Am. B*, 8, 1634-1641, (1991).
- 6 V.A. Bogatyrev et al.: *IEEE J. of Lightwave Technol.*, 9, 561-565, (1991).
- 7 S.V. Chernikov, D.J. Richardson, R.I. Laming, E.M. Dianov, D.N. Payne: *Electron. Lett.*, 28, 1220-1221, (1992); S.V. Chernikov, J.R. Taylor: *Electron. Lett.*, 28, 931-932, (1992).
- 8 S.V. Chernikov, D.J. Richardson, R.I. Laming, E.M. Dianov and D.N. Payne: *Electron. Lett.*, 28, 931-932, (1992).
- 9 D.J. Richardson, R.P. Chamberlain, L. Dong, D.N. Payne, A.D. Ellis, T. Widdowson and D.M. Spirit: *Electron. Lett.*, 31, 470-472, (1995).
- 10 A.D. Ellis, W.A. Pender, T. Widdowson, D.J. Richardson, L. Dong, R.P. Chamberlain: *Electron. Lett.*, 31, 1362-1364, (1995).
- 11 D.J. Richardson, R.P. Chamberlain, L. Dong, D.N. Payne: *Electron. Lett.*, 31, 1681-1682, (1995).
- 12 See e.g. B.J. Ainslie and C.R. Day: *IEEE J. of Lightwave Technol.*, 8, 967 (1986). A.W. Snyder and J.D. Love: *Optical Waveguide Theory* (Chapman and Hall, 1983).
- 13 S.V. Chernikov, J.R. Taylor and R. Kayshap: *Opt. Lett.*, 19, 539-542, (1993).
- 14 E.A. Swanson, S.R. Chin, K. Hall, K.A. Rauschenbach, R.S. Bondurant and J.W. Miller: *Technical Digest Optical Fibre Communications, Postdeadline paper, PD15-1* (San Jose, 1994).
- 15 A.D. Ellis, T. Widdowson, X. Shan, G.E. Wickens, D.M. Spirit: *Electron. Lett.*, 29, 990-991, (1993).
- 16 K. J. Blow and N.J. Doran: *Photon. Tech. Lett.*, 3, 369-371, (1991).
- 17 A. Hasegawa and Y. Kodama: *Opt. Lett.*, 15, 1443-1445, (1990).
- 18 N.J. Smith, K.J. Blow and I Andonovic: *J. Lightwave Technol.*, 10, 1329-1333, (1992).
- 19 L. Treitinger et al.: *Proceedings European Conference on Optical Communications, Vol.1, Paper Tu.A.2.2*, 189, (Brussels, 1995).
- 20 J. P. Gordon, H.A. Haus: *Opt. Lett.*, 11, 665-667, (1986).
- 21 L.F. Mollenauer, J.P. Gordon, and S.G. Evangelides: *Opt. Lett.*, 17, 1575-1577, (1992)
- 22 M. Nakazawa, E. Yamada, H. Kubota, and E. Suzuki: *Electron. Lett.*, 27, 1270-1271, (1991).
- 23 L.F. Mollenauer, J.P. Gordon and M.N. Islam: *IEEE J. Quantum Electron.*, QE-22, 157-173, (1986).
- 24 M. Nakazawa and Kurokawa K.: *Electron. Lett.*, 27, 1369-1371, (1991).
- 25 A.F. Evans, A.J. Stentz and R.W. Boyd: *Proceedings European Conference on Optical Communications ECOC'94, Vol.1*, 323-326 (Florence, 1994).
- 26 A.J. Stentz, R.W. Boyd and A.F. Evans: *Opt. Lett.*, 20, 1770-1772, (1995).